2025 IEEE/SICE International Symposium on System Integration (SII)
January 21-24, 2025, Munich, Germany

Versatile Robotic System for Assembly Tasks Using Flexible Mechanism

Masanori Ueda[1], Ryunosuke Yamada[1], Tokuo Tsuji[2], Kaihei Okada[1], Takehiro Nishimura[1], Ryota Shimizu[1], Yuya Otsu[1], Kaori Yoshino[1], Yosuke Suzuki[2], Toshihiro Nishimura[2] and Tetsuyou Watanabe[2]

***Abstract*— We propose an assembly system involving two robotic arms with flexible mechanisms. These flexible joints provide passive compliance, allowing the robots to absorb positional errors between assembly parts and their respective destinations. Our machine learning-based object detection system shows robustness against variations in color, shape, and ambient lighting, achieving high positional accuracy. This system achieves the execution of diverse assembly tasks using a single setup, facilitated by a universal gripper and machine learning capabilities. Furthermore, the flexible joints minimize the need for precise trajectory planning. In our study, we implemented both an instruction support system and a position error correction system using object detection. We conducted real-world assembly experiments to evaluate these systems, focusing on tasks such as screw tightening and belt drive assembly, with alignment achieved through vision feedback and force feedback control.**

I. INTRODUCTION

The installation of industrial robots for automated assembly tasks addresses worker shortages in factories and enhances productivity. Assembly tasks are inherently complex due to the high level of difficulty, and frequent failures caused by errors in the positioning of parts and holes. Current industrial robots have solved this challenge using standardized operations with jigs and teaching. However, these methods require the design and preparation of jigs and teaching protocols tailored to each part's shape and type. Additionally, a suitable hand or gripper is necessary for each part, increasing the need for multiple hands as the variety of parts grows. This replacement process also takes time. In factories with industrial robots, robots have typically replaced only part of the work. Introducing robots requires creating operations that consider coordination with human production lines, which increases manufacturing costs. Consequently, product prices rise, and integrating robots into existing production lines is time-consuming. This complexity makes it difficult to respond flexibly and promptly to frequent product improvements or customizations.

We have proposed an assembly system robust to positional errors using grippers with flexible mechanisms and feedback control with cameras and force sensors [1] [2]. Object detection using camera images involved image processing techniques such as binarization, template matching, and Hough transformation, but these were susceptible to the shape and color of the object and the influence of ambient light. Additionally, the flexible mechanism was either large or reduced in size by limiting it to 2 degrees of freedom, and there was a trade-off between the size of the mechanism and its degrees of freedom. Furthermore, because the flexible mechanism is attached to the base of the gripper, there was a problem that the extremity of the hand droops due to gravity when the hand is turned sideways.

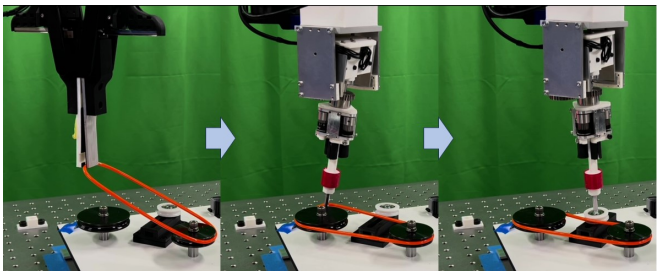

Fig. 1: Overall robot system and belt drive appearance. Assemble the belt drive with simple force feedback control by flexible mechanisms.

Therefore, we implement an object detection using YOLOv7 [3], which is a machine learning method, and a gripper with a small, flexible joint securing 6 degrees of freedom, and propose an assembly system that is robust to positional errors. Compliance control is a method for absorbing positioning errors between assembly parts and their assembly locations, providing robots with elastic properties [4]. It can be broadly divided into two types: active compliance control [5], which changes stiffness by the robot's own control, and passive compliance record, which introduces flexible mechanisms. Active compliance control requires advanced actuators and sensors, whereas passive compliance control can be achieved with just the mechanism, allowing for miniaturization and simplification of the mechanism. Therefore, we focus on passive compliance control and incorporated flexible joints with six degrees of freedom in each of the two robot arms according to their respective purposes. Machine learning-based object detection is less affected by the shape and color of the image and the surrounding light, and detect the position of objects with high accuracy. YOLOv7 has high real-time performance and achieve fast camera feedback control. Moreover, we develop a teaching system that

[1] M. Ueda, R. Yamada, K. Okada, T. Nishimura, R. Shimizu, Y. Otsu and K. Yoshino are student of Graduate School of Natural Science and Technology, Kanazawa University, Kakuma-machi, Kanazawa-shi, Ishikawa 920-1192, Japan. masanoriueda0317, noboriryuu0623, kaihei2112, takehiro-92-188, ryota.shimizu, otsuy0525, haru0803@stu.kanazawa-u.ac.jp

[2] T. Tsuji, Y. Suzuki, T. Nishimura, and T. Watanabe are with Faculty of Frontier Engineering, Institute of Science and Engineering, Kanazawa University, Kakuma-machi, Kanazawa-shi, Ishikawa 920-1192, Japan. tokuo-tsuji, suzuki, tnishimura, twata@se.kanazawa-u.ac.jp

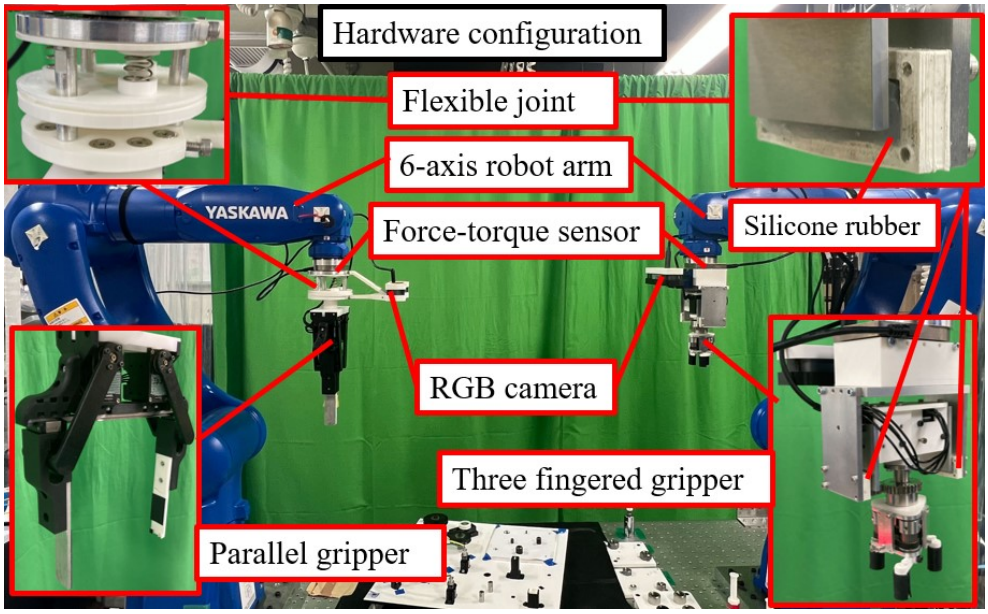

Fig. 2: Hardware configuration of the proposed robot system. The robot system consists of two 6-axis industrial robots, each equipped with a parallel gripper and a three-finger gripper. Between the grippers and the robot arms, there are force sensors, flexible joints, and RGB cameras.

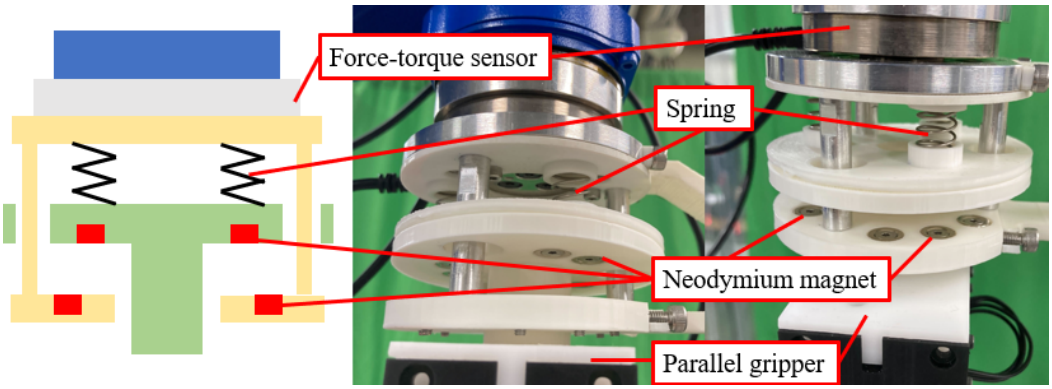

Fig. 3: Overview of the flexible wrist of the parallel robot. The flexible wrist consists of an upper plate, a middle movable plate, and a lower plate. The middle movable plate is connected to the upper plate by three springs and to the lower plate by six and nine neodymium magnets in a repelling orientation, respectively.

incorporates machine learning, enabling users to easily teach object positions. Robot systems for automatic assembly tasks have also been developed. Notably, research has focused on object detection systems for peg-in-hole tasks, employing both vision-based [6] and contact-based [7] [8] approaches. Huges *et al.* [9] have proposed a system using convolutional neural networks for object detection as a general assembly system. We propose a more robust system by using YOLOv7 for object detection to achieve fast vision feedback control, and by further using flexible joints.

We evaluate the effectiveness of the proposed system through the system benchmark proposed by Kimble *et al.* [10], focusing on screw tightening and belt drive assembly of the Fig. 1. The belt drive was also adopted in the industrial robot competition at the World Robot Summit 2018 (WRS2018) [11], and is widely known as a benchmark for assembly systems. The belt drive assembly first involves placing the belt on two pulleys, then it is necessary to move the idler pulley to tension the belt. Since the idler pulley is bolted in place, it is necessary to tighten or loosen the bolt. Operational strategies for belt drive assembly have been proposed in previous research. Nishimura *et al.* [12] performed belt drive assembly with a timing belt using a single gripper and evaluated the success rate of the assembly work. Jin *et al.* [13] have proposed trajectory optimization for belt assembly, all of which are assembly tasks performed by highly rigid robot systems. Additionally, since the belt is made of a flexible material and there is a possibility of assembly failure even with precise teaching, the manipulation of deformable objects by robots has been extensively studied, as surveyed by Sanches *et al.* [14]. In our study of belt drives, using bolts to secure the idler pulley complicates the assembly process.

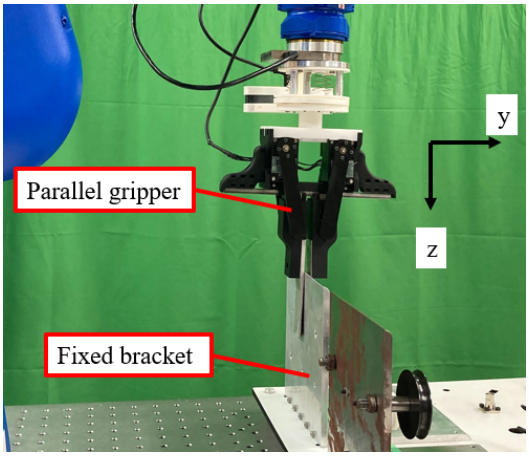

Fig. 4: Experimental measurement of the flexibility of the wrist in the parallel robot. The changes in the amount of movement and force perception of the robot in the y-axis direction were measured when a load was applied in the z-axis direction, when no load was applied, and when there was no flexible wrist.

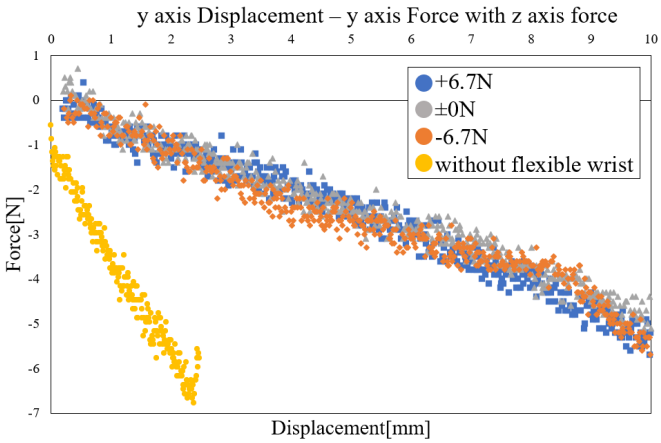

Fig. 5: Results of the flexibility experiment. Regardless of the load in the z-direction, it can be seen that flexibility is maintained. It can also be seen that the introduction of flexible joints has reduced the force values relative to the amount of movement.

Furthermore, assembly tasks are performed with a versatile gripper, so that it can also be used for other tasks such as peg-in-hole assembly and wire connecting.

II. Hardware Configuration

A. Overview

The overall configuration of the proposed robot system is shown in Fig. 2. Each of the two 6-axis industrial robots (MOTOMAN-GP7, YASKAWA) is equipped with a parallel gripper and a three-finger gripper at the end of their arms. A robotic arm featuring a parallel gripper was called a parallel robot. Conversely, one with a three-finger gripper was called a chuck robot due to the movement of its fingers. Between the grippers and the robot arms, there are force sensors (FFS055YS102U6_S055F103, Leptrino, frequency 10ms) , flexible joints, and RGB cameras (C1000eR, Logicool BRIO, resolution 3840×2160, fps 30).

B. Flexible Joint

Flexible joint has been introduced according to each gripper. A flexible wrist consisting of springs and permanent magnets has been introduced in parallel robots. This flexible wrist in the top left of Fig. 2 ensures 6 degrees of flexibility, and although it is not suitable for work in the horizontal direction of the hand, it can handle loads from other directions due to the non-contact flexibility of the permanent magnets. Fig. 3 shows this flexible wrist in greater detail. A force sensor is installed under the robot's hand, and below that, the flexible wrist is installed.

The left side of Fig. 3 schematically shows a flexible wrist. There is a plate that can move between the upper plate connected under the force sensor and the lower plate connected by a support. This plate is called a middle movable plate. Between the middle moving plate and the upper plate, three springs are installed, and on the middle moving plate and the lower plate, six and nine neodymium magnets are installed in a repelling orientation, respectively. To ensure 6 degrees of flexibility, holes are made in the middle moving plate sufficiently large to avoid interference with the pillars. Using magnets ensures flexibility without contact and reduces friction, so flexibility in other directions does not change even when a load is applied in one direction. When the flexible wrist was constructed with only magnets, the positional stability of the gripper became a problem, so springs were introduced at the top. The chuck robot uses flexible joints made of silicone rubber to connect the gripper part and the robot arm part. These flexible joints are positioned near the center of gravity of the gripper as shown in the upper right of Fig. 2, preventing the fingertips from drooping due to gravity when the hand is horizontal. Additionally, the silicone rubber, while being very compact, ensures flexibility with 6 degrees of freedom.

C. Flexibility of the wrist of the parallel robot

To verify the flexibility of a flexible wrist, we measured the change in the robot's movement and force-torque perception values when a load was applied to the flexible wrist, when no load was applied, and when there was no flexible wrist. The experimental setup is shown in Fig. 4. A fixed obstacle was firmly gripped with a gripper, and a load was applied in the z-axis direction by pushing and pulling from that state. Afterwards, the robot was moved at a constant speed in the y-axis direction, and the amount of movement and force sensation values were measured. The graph of the experimental results is shown in Fig. 5. Regardless of the load in the z-direction, the flexibility is maintained. The introduction of flexible joints has effectively lowered the force associated with the amount of movement. The flexible wrist suppress the sudden increase in force perception when loaded, thereby enhancing the robot's safety and controllability. From Fig. 5, it is also apparent that flexibility is maintained regardless of the load

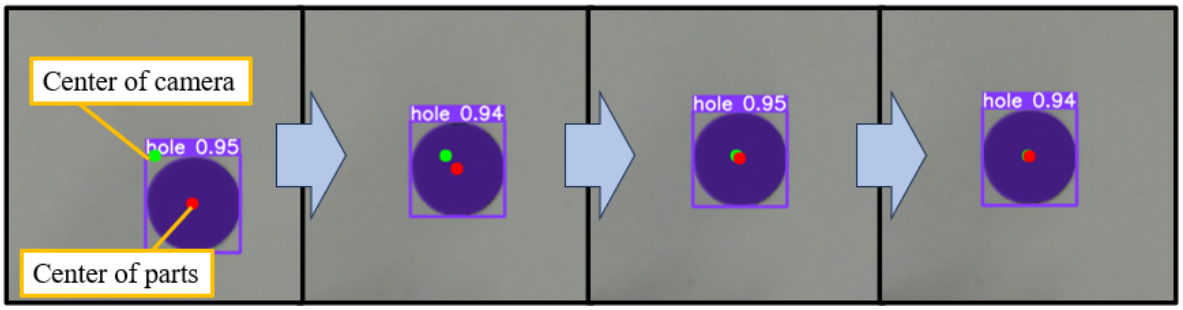

Fig. 6: Adjust system with object detection. Green represents the center of the camera, and red represents the center of the object. The robot moves to adjust the object to the center of the camera.

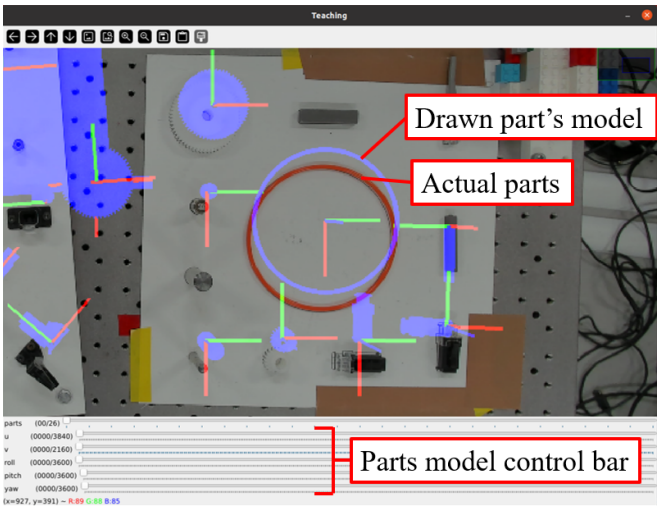

Fig. 7: GUI of the teaching system. The user can teach the position and posture of the object by clicking on the image or draging the bar.

in the z-direction. When the belt is pulled, flexibility in other directions is also ensured. This improves the operability of belt drives compared to RCC devices [15].

D. Gripper

In the lower left of Fig 2, the gripper of the parallel robot incorporates a mechanism similar to the gripper developed by Tennnomi *et al.* [1]. The gripper of the chuck robot in the bottom right of the figure is a three-fingered gripper, and the opening and closing of the fingers are performed by rotating the shafts mounted at the base of each finger. By inputting into a differential mechanism with two motors, it is possible to perform the opening and closing of the fingers and the infinite rotation of the palm by switching each rotation.

III. Software Configuration

A. Control System

Choreonoid [16] on Ubuntu 20.04 was used for a robot development platform. Choreonoid is software for robot modeling, simulation, and control. In Choreonoid, robots are drawn through a graphical user interface (GUI), and execute via Python scripts in a character user interface (CUI) is also possible. We developed a plugin in C++ as an extension of Choreonoid, enabling robot control from Python scripts through the API. Object detection by machine learning, force values from force sensors, image acquisition from cameras, and robot commands are all done through ROS2 [17] from Choreonoid.

B. Vision System

As shown in Fig. 2, the process of capturing images and detecting objects is conducted using RGB cameras attached to each gripper. These cameras were strategically positioned away from the central axis of the gripper to avoid interference with the hands. The spatial relationship between the hands and the cameras was established through hand-eye calibration [18].

C. Object Detection System

For the object detection system, YOLOv7 instance segmentation was used. When the name of the part to be detected is received from Choreonoid, images from the camera are received via ROS2. Object detection is performed on a computer with RTX 4060Ti GPU on Ubuntu 20.04, and the center coordinates of the detected object's image coordinate system are transmitted to Choreonoid via ROS2. Object detection was mainly used for the fine-tuning of robots and the teaching systems. In robot fine-tuning, the distance between the camera center and the object in the world coordinate system is calculated by calculating the camera position from the robot's joint angles and the object position in the image coordinate system obtained from the object detection system. As shown in Fig. 6, if green represents the center of the camera and red represents the center of the object, the distance between the center of the object and the camera is multiplied by a coefficient from 0 to 1, and the camera center is moved several times without exceeding the object center to align the centers.

D. Teaching System

The teaching system is a system for users to accurately instruct the position of an object based on the position of the object obtained from the object detection system. The teaching system consists of a GUI as shown in Fig. 7. It projects the model of the object at the location of the object detected by the object detection system on the image received

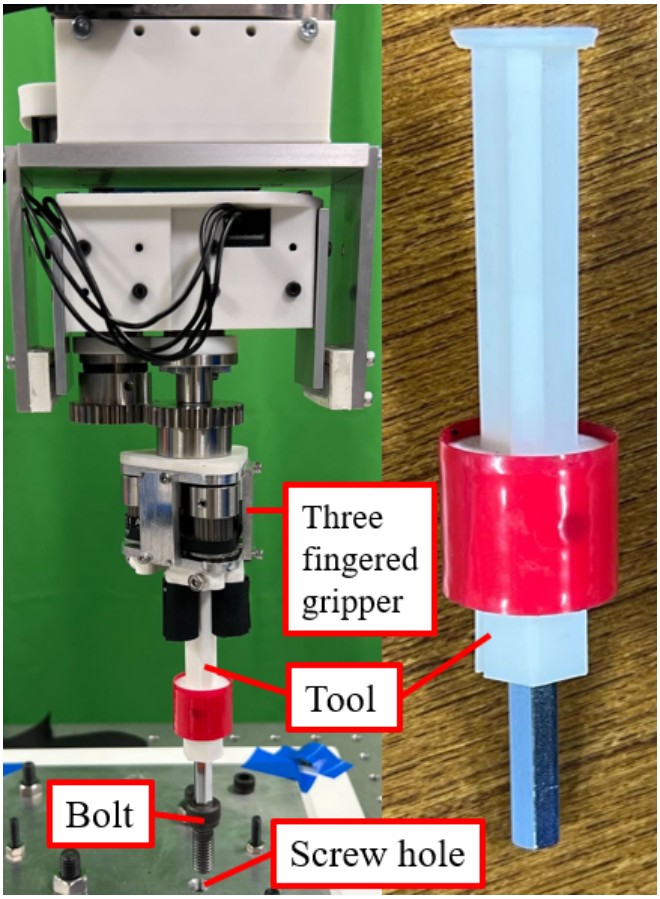

Fig. 8: Experimental setup for screw tightening. The chuck robot tightens the screw while measuring the torque and tightening direction force. The tool is without an actuator, allowing for low-cost tightening of screws of various sizes.

from the camera. In the object detection system, there is a slight positional error and since it does not detect posture, it allows the user to accurately teach the position of the object from there. The position and orientation of the model of the object drawn are changed by clicking on the image, dragging the bar at the bottom, or by keyboard operations. After the adjustments, the position and orientation of the drawn object in the image coordinate system are converted into the position and orientation in the world coordinate system and transmitted to Choreonoid.

IV. Assembly Tasks

The proposed system was evaluated by performing screw tightening using the chuck robot and belt driving by both robots. The tasks used are parts of the benchmark for the automated assembly system proposed by Kimble *et al.* .

A. Screw Tightening method

In screw tightening, after aligning the screw and the screw hole using the object detection system. Next, the torque and tightening direction force generated when the chuck robot tightens the screw are measured, and it is determined whether to further push the robot or if the screw tightening is

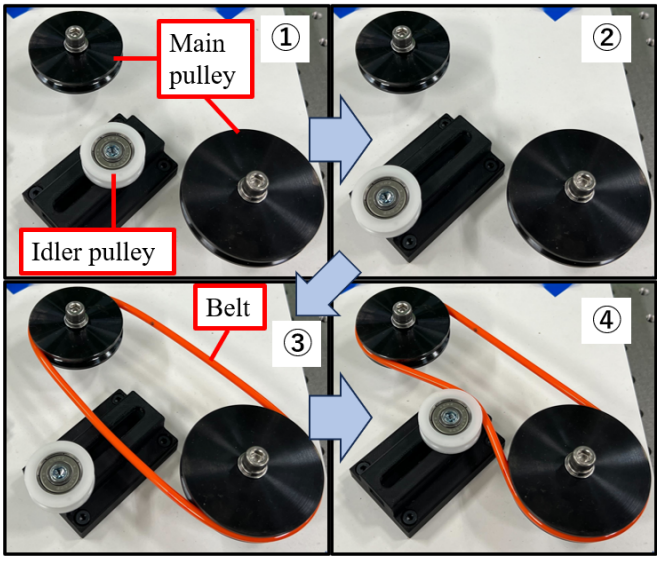

Fig. 9: Belt drive assembly. There are two main pulleys and an idler pulley on the slider between them. First, removing the idler pulley, then hooking the belt to the main pulleys. Finally, moving the idler pulley to tension the belt.

complete. First, perform alignment with the object detection system. Use tools like those in Fig. 8, detect bolts attached to the tip using template matching, and compare their position with the position of screw holes detected by YOLOv7. After the robot approaches the position where the bolt tip overlaps with the screw hole as seen from the camera, it completes the alignment by moving the distance of the radius of the screw hole and the radius of the screw.

The screw is initially driven at a high rotational speed. Once the applied force surpasses a predefined threshold, the speed is decreased to securely fasten the screw. The infinite rotation function of the palm eliminates the need for a rotary tool with an actuator, allowing for low-cost tightening of screws of various sizes. While gripping and rotating the tool, if the detected force in the direction of the screw hole drops below a certain value, the robot applies force in the pushing direction. During slow rotation, in addition to this program, if the torque in the tightening direction exceeds a certain value, it is determined that the tightening is complete.

B. Screw Tightening Experimental

Using the aforementioned system, screw tightening experiments were conducted. The screws were M8 hex bolts, with a length of 20mm. Twenty tightening experiments were carried out, and the success rate was measured.

As a result, all trials were successful, and the average time required was 32.9 seconds. In addition, the standard deviation was 8.53 seconds. As a reason for the increase in standard deviation, when retracting the tool after tightening the screw, it is necessary to appropriately rotate the tool by force feedback so that it does not catch on the bolt hole, but this operation caused variability.

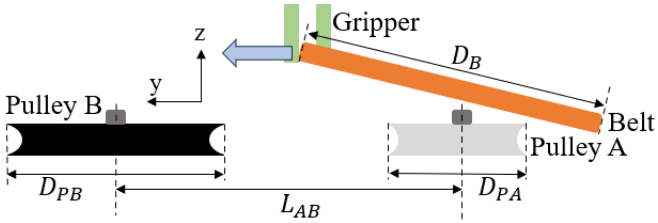

Fig. 10: Schematic of the hooking process. The belt is hooked onto the pulley A at first, and then hooked onto the pulley B.

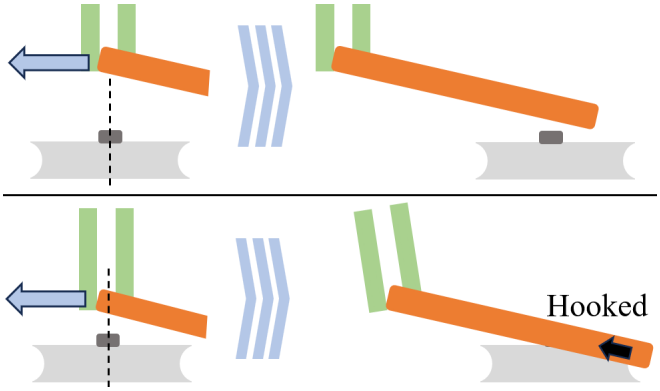

Fig. 11: Force and moment data obtained when hooking the belt. If the moment value does not exceed a certain level, lower it slightly in the z-direction and perform the hooking operation again.

C. Belt Drive Assembly

As shown in Fig. 9, the belt drive has two main pulleys and an idler pulley on the slider between them. Before placing the belt on the main pulleys, it is necessary to loosen the screw of the idler pulley and move it over the slider. After installing the belt, move the idler pulley so that it tightens the belt, and then tighten the central screw. When loosening the screws of the idler pulley, use a chuck robot holding a tool and align the robot with the bolt holes using the screw tightening method described in Section 4A.

1) Idler pulley removal: Loosen the screw in the center of the idler pulley, and move the slider carrying the idler pulley away from the y-axis while the tool remains stuck in the screw hole. This move the idler pulley from the position where the belt is likely to be applied.

2) Hooking the Belt to the pulley A: After moving the chuck robot to a safe place, the parallel robot is used to grip the belt. Place the belt on one of the main pulleys and hook it onto the screw hole at the top of the other main pulley with the parallel robot. First, designate the main pulley on which the belt is initially placed as pulley A, and the other as pulley B. Set a coordinate system with the line connecting the center points of pulley A and pulley B as the y-axis, the vertical direction as the z-axis, and the center point of pulley A as the origin. As shown in Fig. 10, the diameter of pulley A is denoted as D_{PA}, the diameter of pulley B as D_{PB}, the distance between the centers of pulley A and pulley B as L_{AB}, and the circumferential diameter of the belt as D_B. Move the robot from pulley A towards pulley B, and if the moment around the x-axis exceeds a certain value, it is determined that the belt is applied to pulley A. If it does not exceed a certain value, return to the state before moving towards pulley B, move a little in the negative z-direction, and repeat this action. As shown in Fig. 11, the initial position of the gripper before moving the belt is above the center of pulley A. Since the belt is flexible, the unheld tip side is easily deflected by its own weight, and the amount of deflection changes depending on how it is gripped. Therefore, the starting position needs to be sufficiently above the center of pulley A.

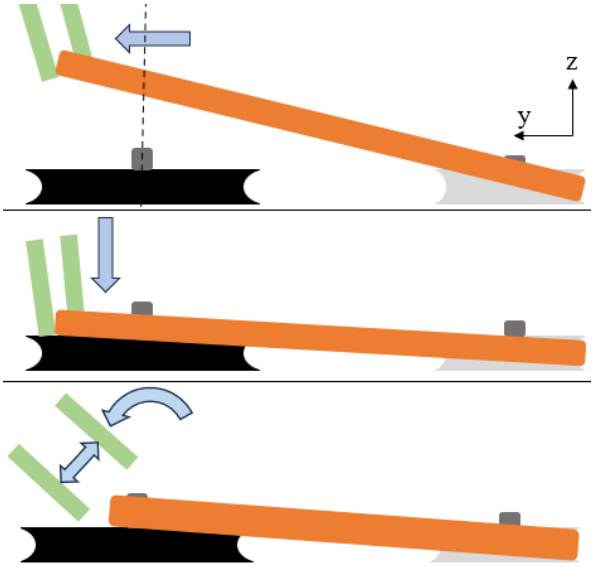

Fig. 12: Move the robot straight down until it detects force values, and open the gripper to hook the belt onto the head of screw on the pulley B. After that, use the chuck robot to easily hook the belt into the groove of pulley B.

3) Hooking the Belt to the pulley B: After the belt is placed on pulley A, it is hooked onto pulley B. The belt is held by the parallel gripper, and because it is difficult to directly hook it onto the groove of pulley B, the chuck robot is used with a tool to hook the belt. Therefore, as the belt needs to be kept on pulley A while using the tool, it is possible to work safely by hooking the belt onto the bolt head of pulley B as shown in Fig. 12.

Next, completely hook the belt onto pulley B with the chuck robot. By using the tool used to remove the idler pulley, it is possible to save the time of changing tools. First, insert the tool at the midpoint between pulley A and pulley B and move while checking the moment value as shown in Fig. 13, to find the approximate intersection of the belt and the pulley. After reaching the intersection of the belt and the pulley, the belt is hooked into the groove by rotating the gripper around the center of pulley B. The rotation radius at this time is set to be the same as the radius of pulley B, but even if there is some error, the belt can be hooked into the groove by the flexible joint.

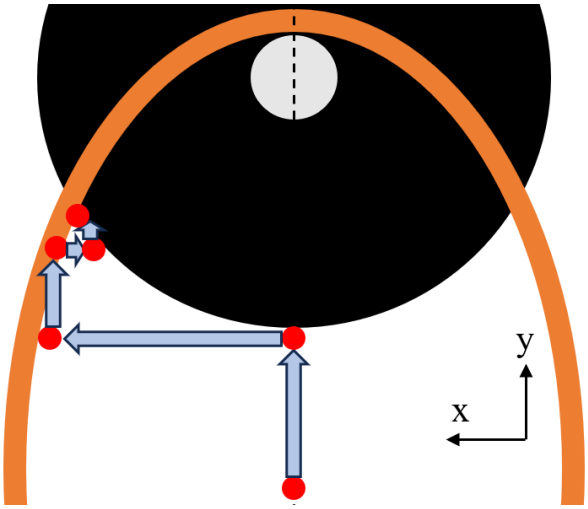

Fig. 13: Searching for the intersection of the belt and pulley B by force-torque feedback. After reaching the intersection, the robot moves rotating around the center of the pulley B.

4) Idler pulley installation: After placing the belt on both pulleys, move the idler pulley that was set aside so that it tightens the belt, and tighten the central screw. Whether the belt is tight is determined by force-torque feedback.

D. Belt Drive Assembly Experimental

Using the previously mentioned assembly algorithm, an assembly experiment of a belt drive was conducted. The belt used has a diameter of 4mm and a circumferential diameter D_B of 120mm. The center-to-center distance between pulley A and B is L_{AB}=115mm. The diameters of pulley A and pulley B are D_{PA}=62mm and D_{PB}=50mm, respectively.

We conducted 20 assembly experiments and measured their success rate. We successfully applied tension to the belt 18 times and failed to apply tension twice. In the 18 successful trials of applying tension to the belt, the average time required was 244.83 seconds. The standard deviation was 6.54 seconds. When inserting the tool into the bolt hole of the idler pulley to apply tension and tighten the screw, the tool fell off during rotation because the tool's posture was too tilted. The flexible joints introduced in this robotic system are incapable of changing their flexibility. For tasks where posture is important, it is preferable to have joints with high rigidity, therefore, introducing flexible joints with variable stiffness can be considered as a future improvement.

V. Conclusion

In this study, we proposed an automatic assembly system using two robotic arms equipped with flexible joints. In this system, we implemented object detection by machine learning, an instructional support system utilizing it, and a position error correction system, and conducted actual assembly experiments with these systems. Additionally, by using feedback control via force sensors, experiments on belt drive assembly were conducted, demonstrating successful assembly even without precise motion creation through flexible joints. The flexible wrist of the parallel robot uses magnets to ensure flexibility without contact, reducing friction and demonstrating that it can handle loads from multiple directions, such as during belt tensioning. We improved the flexibility of joints from the conventional system, succeeded in assembling the belt drive, and enhanced robustness by switching the vision system to a machine learning base.

References

[1] M. Tennomi, A. Okamura, Y. Nakamura, T. Abe, S. Wakamatsu, S. Tajima, T. Nishimura, Y. Hirai, T. Sawada, N. Ichikawa, T. Tsuji, K. Yamazaki, Y. Suzuki, and T. Watanabe, "Development of assembly system with quick and low-cost installation," *Advanced Robotics*, vol. 34, pp. 531 – 545, 2020.

[2] K. Tabata, T. Tsuji, A. Kawakubo, R. Kobayashi, T. Yamabe, Y. Suzuki, T. Nishimura, K. Yamazaki, T. Ishiti, and T. Watanabe, "Integrating force and vision feedback for flexible assembly system," in *Advanced Robotics*, vol. 37, no. 17, 2023, pp. 1100–1111.

[3] C.-Y. Wang, A. Bochkovskiy, and H.-Y. M. Liao, "Yolov7: Trainable bag-of-freebies sets new state-of-the-art for real-time object detectors," 2022.

[4] K. Kuo and J. Lin, "Fuzzy logic control for flexible link robot arm by singular perturbation approach," *Applied Soft Computing*, vol. 2, pp. 24–38, 08 2002.

[5] Y. Gai, J. Guo, D. Wu, and K. Chen, "Feature-based compliance control for precise peg-in-hole assembly," *IEEE Transactions on Industrial Electronics*, vol. 69, pp. 9309–9319, 2022.

[6] F. Chaumette and S. A. Hutchinson, "Visual servo control. i. basic approaches," *IEEE Robotics & Automation Magazine*, vol. 13, pp. 82–90, 2006.

[7] H.-C. Song, Y.-L. Kim, and J.-B. Song, "Guidance algorithm for complex-shape peg-in-hole strategy based on geometrical information and force control," *Advanced Robotics*, vol. 30, pp. 552 – 563, 2016.

[8] M. Hebecker, J. Lambrecht, and M. Schmitz, "Towards real-world force-sensitive robotic assembly through deep reinforcement learning in simulations," *2021 IEEE/ASME International Conference on Advanced Intelligent Mechatronics (AIM)*, pp. 1045–1051, 2021.

[9] J. Hughes, K. Gilday, L. Scimeca, S. Garg, and F. Iida, "Flexible, adaptive industrial assembly: driving innovation through competition," *Intelligent Service Robotics*, vol. 13, pp. 169 – 178, 2019.

[10] K. Kimble, J. Albrecht, M. Zimmerman, and J. Falco, "Performance measures to benchmark the grasping, manipulation, and assembly of deformable objects typical to manufacturing applications," *Frontiers in Robotics and AI*, vol. 9, 2022.

[11] Y. Yokokohji, Y. Kawai, M. Shibata, Y. Aiyama, S. Kotosaka, W. Uemura, A. Noda, H. Dobashi, T. Sakaguchi, and K. Yokoi, "Assembly challenge: a robot competition of the industrial robotics category, world robot summit summary of the pre-competition in 2018*," *Advanced Robotics*, vol. 33, pp. 876 – 899, 2019.

[12] K. Nishimura and H. Dobashi, "Robust assembly strategy of a timing belt in the belt drive unit against its shape uncertainty with a single parallel jaw gripper," *Advanced Robotics*, vol. 36, pp. 450 – 461, 2022.

[13] S. Jin, D. Romeres, A. Ragunathan, D. K. Jha, and M. Tomizuka, "Trajectory optimization for manipulation of deformable objects: Assembly of belt drive units," *2021 IEEE International Conference on Robotics and Automation (ICRA)*, pp. 10 002–10 008, 2021.

[14] J. Sanchez, J. A. Corrales, B. C. Bouzgarrou, and Y. Mezouar, "Robotic manipulation and sensing of deformable objects in domestic and industrial applications: a survey," *The International Journal of Robotics Research*, vol. 37, pp. 688 – 716, 2018.

[15] D. E. Whitney, "Quasi-static assembly of compliantly supported rigid parts," *Journal of Dynamic Systems Measurement and Control-transactions of The Asme*, vol. 104, pp. 65–77, 1982.

[16] S. Nakaoka, "Choreonoid: Extensible virtual robot environment built on an integrated gui framework," *2012 IEEE/SICE International Symposium on System Integration (SII)*, pp. 79–85, 2012.

[17] S. Macenski, T. Foote, B. Gerkey, C. Lalancette, and W. Woodall, "Robot operating system 2: Design, architecture, and uses in the wild," *Science Robotics*, vol. 7, no. 66, p. eabm6074, 2022.

[18] R. Y. Tsai and R. K. Lenz, "A new technique for fully autonomous and efficient 3d robotics hand/eye calibration," *IEEE Trans. Robotics Autom.*, vol. 5, pp. 345–358, 1988.